

Temperature distribution and magnetic field impact on heat flow in laser-heating experiments relevant to MagLIF

K. R. Carpenter, R. C. Mancini
University of Nevada, Reno – Physics department

E. Harding, A. Harvey-Thompson, M. Geissel, K. Peterson, S. Hansen
Sandia National Laboratories

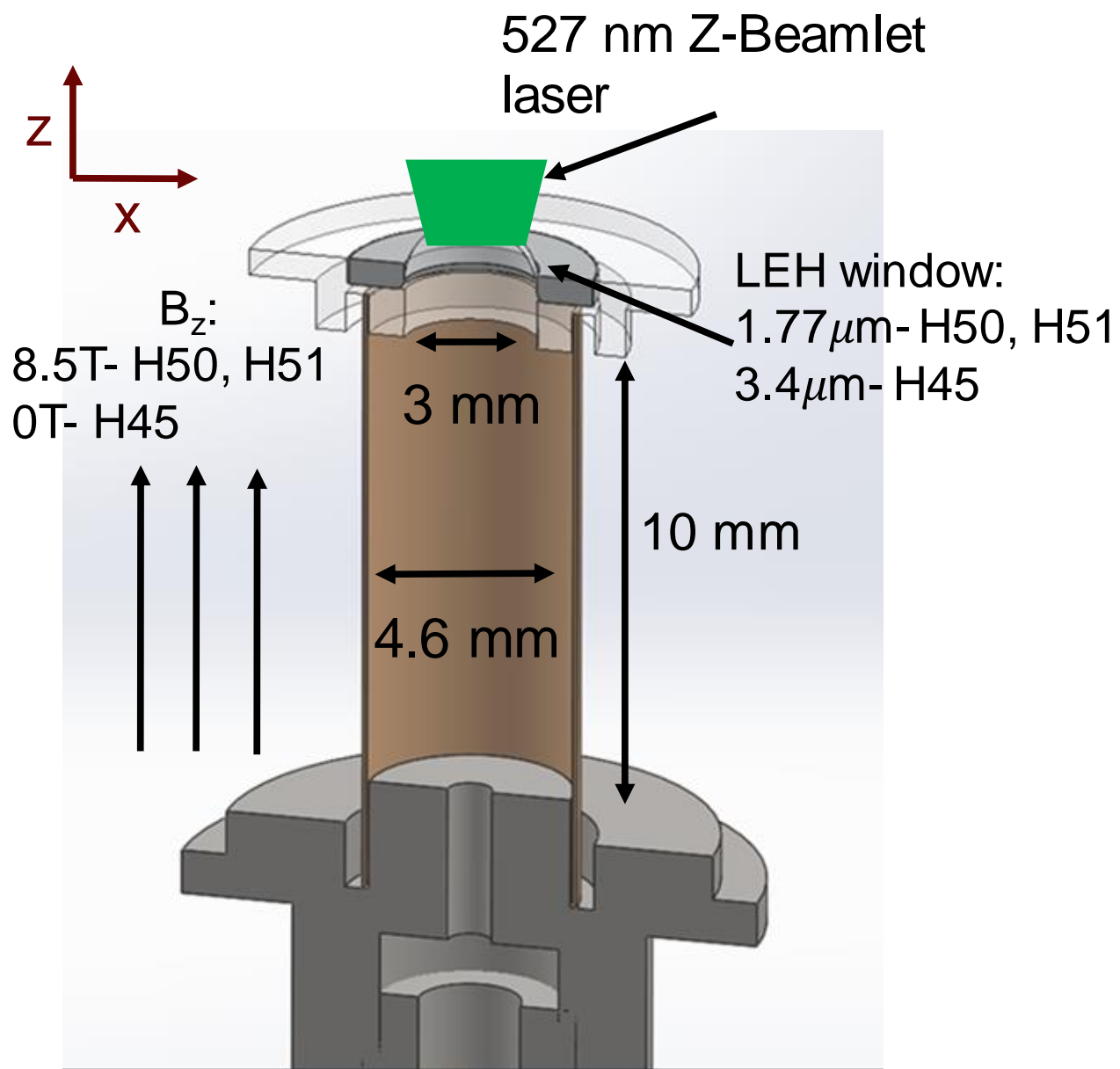
Meeting on Magnetic Fields in Laser Plasmas 2018/04/23

Overview

- Laser heated plasma experiments relevant to Magnetized Liner Inertial Fusion (MagLIF)¹ have been conducted at Z
- Time-integrated spectrum and narrowband image data of Ar K-shell emission were collected during these experiments
- We have analyzed data from two experiments with magnetic field (H45, H50) and one without magnetic field (H51)
- Motivating questions:
 1. What can be extracted from the data and how can it be analyzed?
 2. What physics can we learn from the results?
 3. How can the results be used to plan for future experiments and investigation?

¹S.A. Slutz, M.C. Hermann, R.A. Vesey, A.B. Sefkow, D.B. Sinars, D.C. Rovang, K.J. Peterson, and M.E. Cuneo, Phys. Plasmas **17**, 056303 (2010)

Laser heating experiments at Z



- Be liner target
- Deuterium gas fill (60 psi) doped with 0.1% (atomic) Ar
- Laser pulse heats the fuel, 1 mm diameter focal spot
- Experiments were performed at comparable laser pulse energies
- Time-integrated argon K-shell x-ray emission was observed and can be used for spectroscopy diagnosis
- Experiments with B (H45, H50) and without B (H51) have been conducted and analyzed

Data: B field impacts spectroscopic signatures

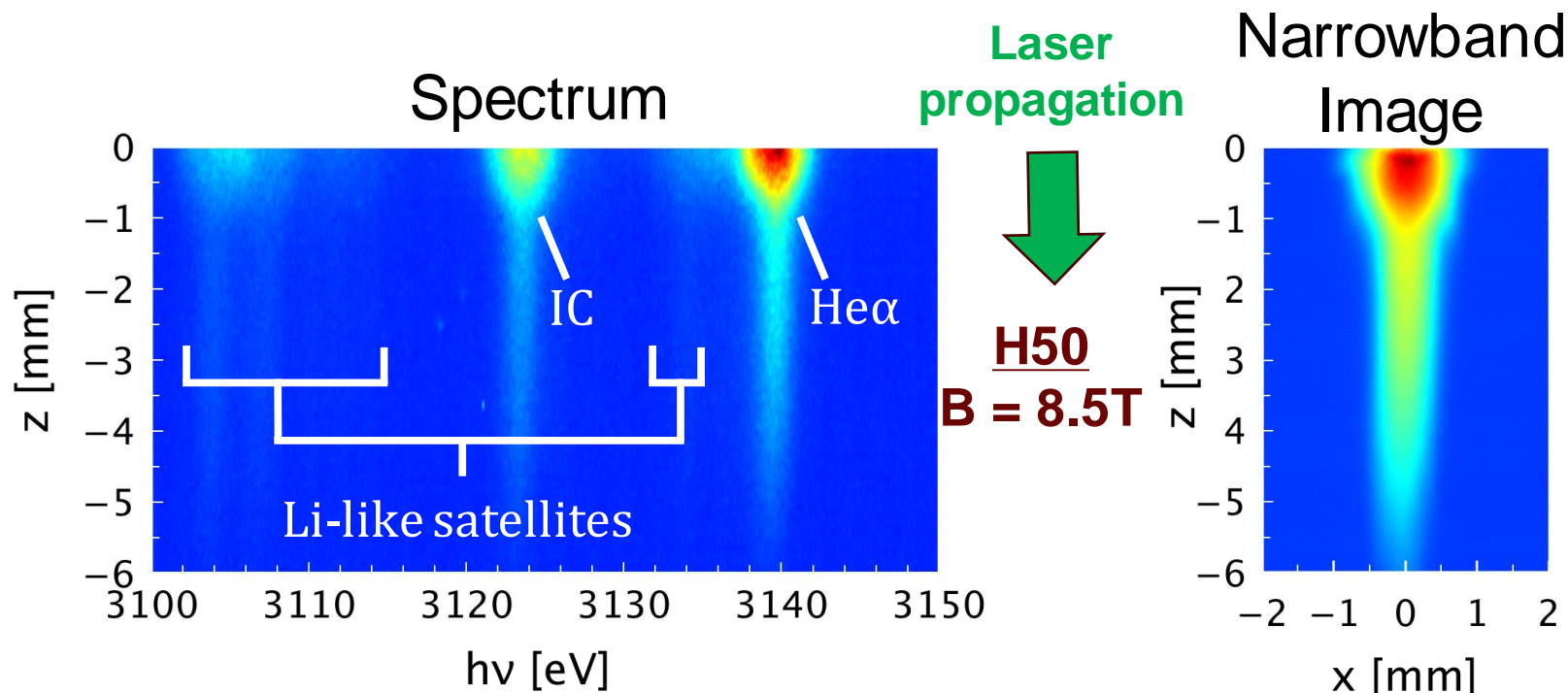
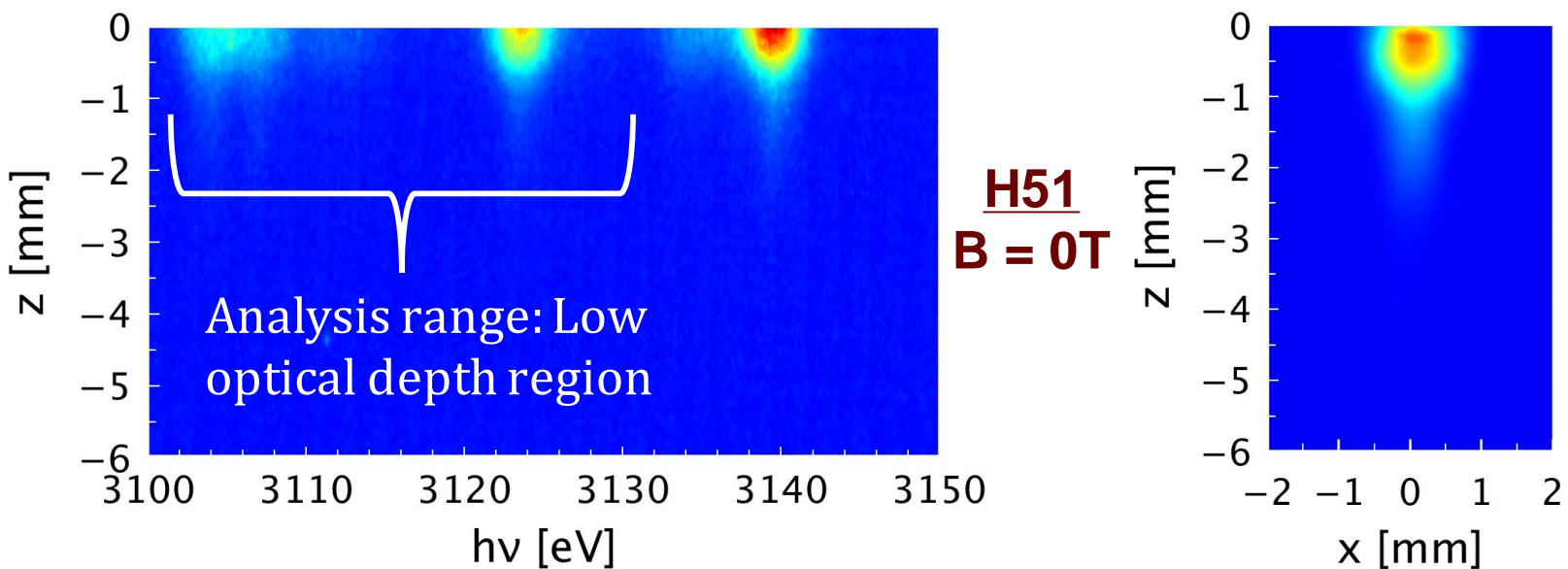


Image characteristics

- Time-integrated
- Axial resolution: 80 μ m
- Transverse resolution: 20 μ m
- $h\nu_0 = 3124\text{eV}$
- $\Delta h\nu = 7.5\text{eV}$

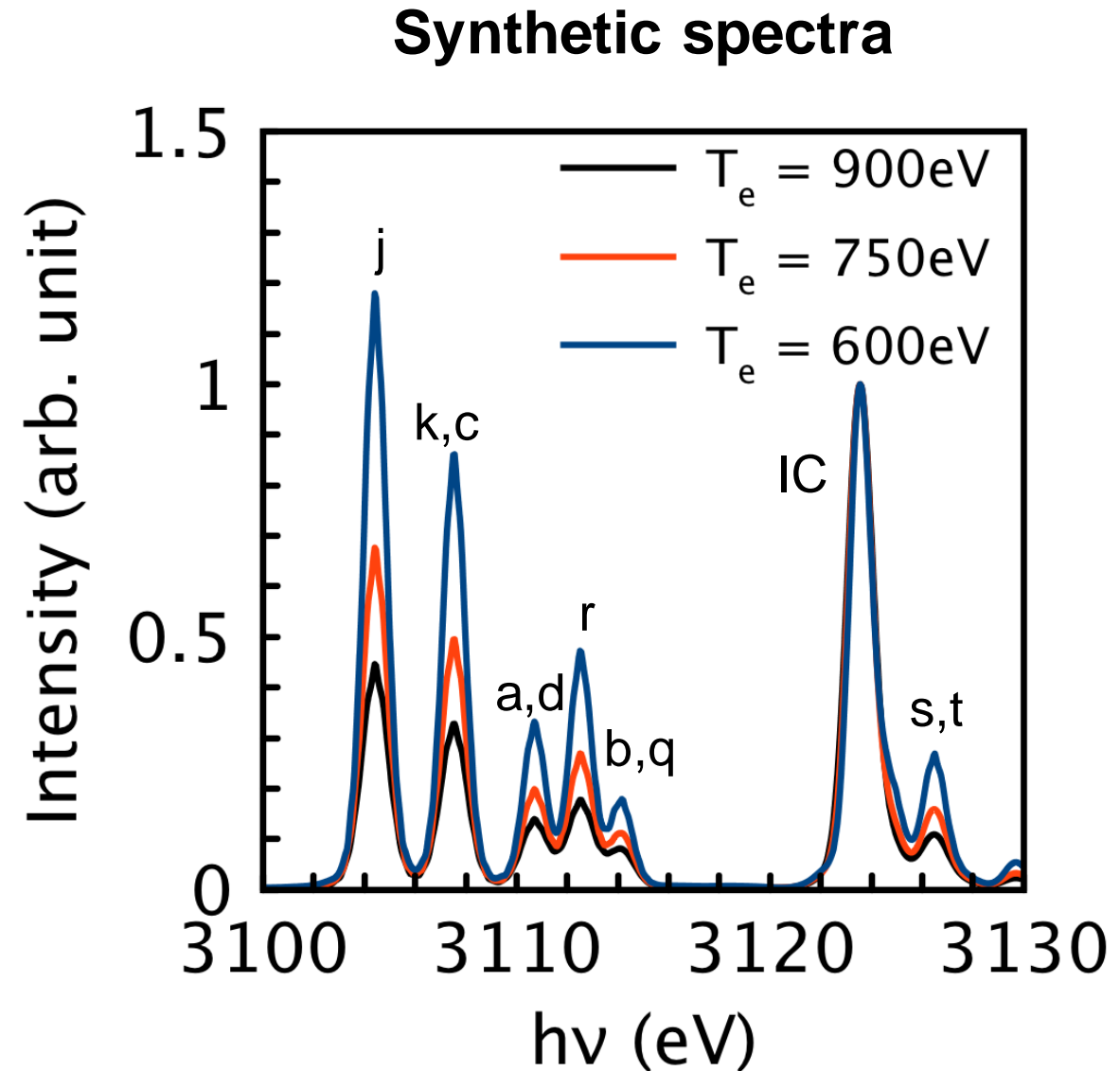


Spectrum characteristics

- Time-integrated
- Observe 2-1 transitions in He-like and n=2 Li-like Ar
- Some Ly α emission in hotter regions of H50
- Axially resolved: $\sim 200\mu\text{m}$
- Spectral resolving power: ~ 1800

Spectra are sensitive to T_e

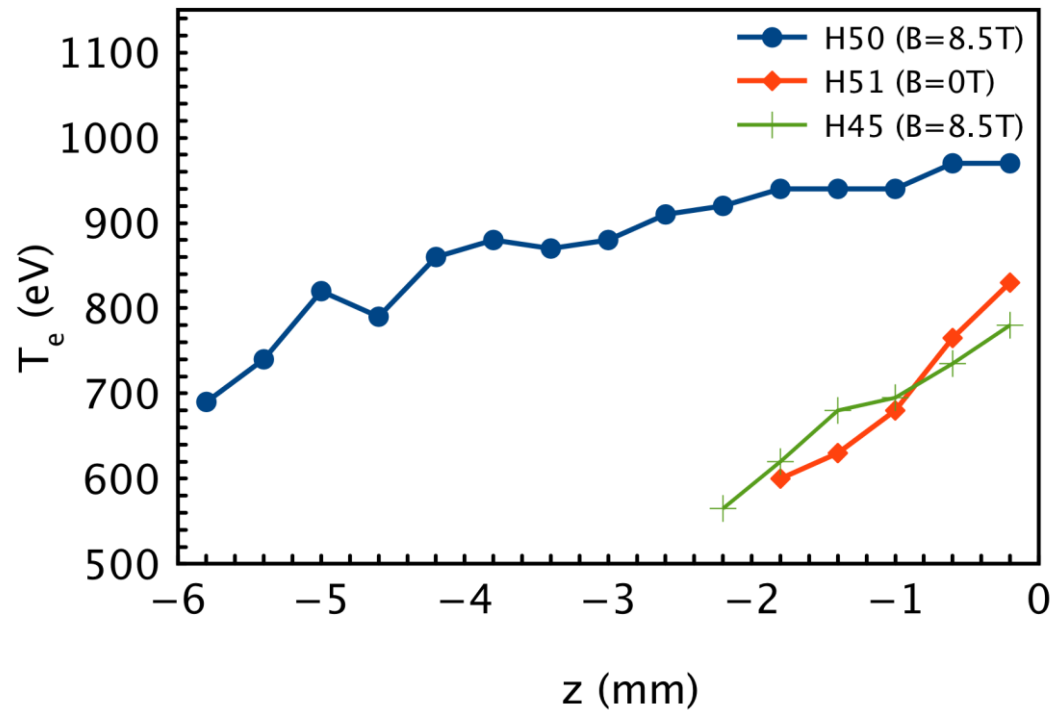
- Ar K-shell model was used to investigate spectrum sensitivity to electron temperature (T_e) and density (N_e)
- NLTE, steady-state simulations of D-Ar plasma produced synthetic spectra
- Important: radiation transport has small effect on the spectral range used for analysis
- PrismSpect¹ was used for the calculation
- Experimental conditions are below threshold of N_e dependence ($\sim 10^{22} \text{ cm}^{-3}$)²
- A constant uniform N_e based on initial conditions and ionization of D is assumed in our analysis ($2.0 \times 10^{20} \text{ cm}^{-3}$)



¹J. J. MacFarlane, I. E. Golovkin, P. Wang and P. R. Woodruff, High Energy Density Physics 3, 181 (2007)

²V.L. Jacobs, J.E. Rogerson, M.H. Chen, and R.D. Cowan, Physical Review A 32, 3382 (1985)

Analysis of axially resolved spectra produces $T_e(z)$

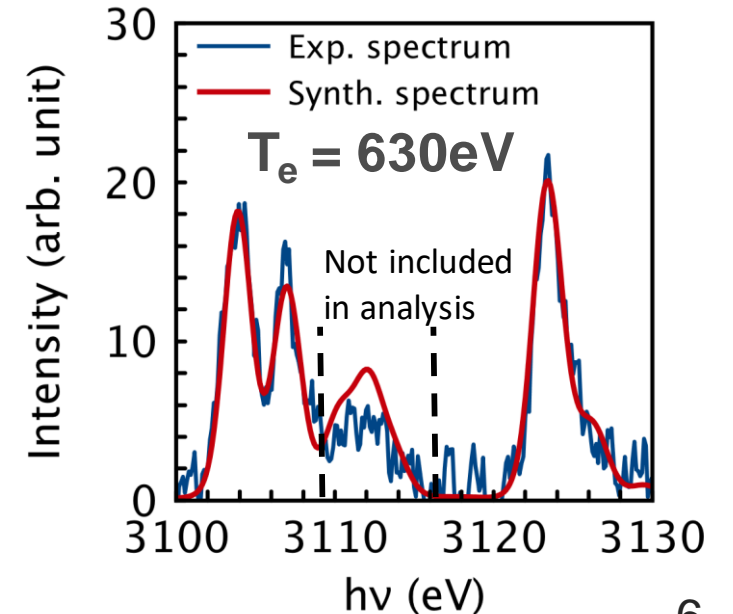
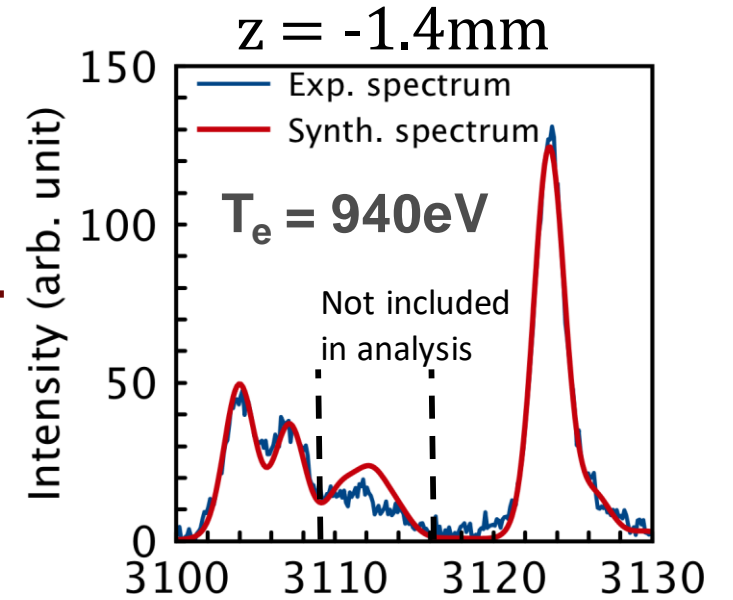


Laser propagation ←

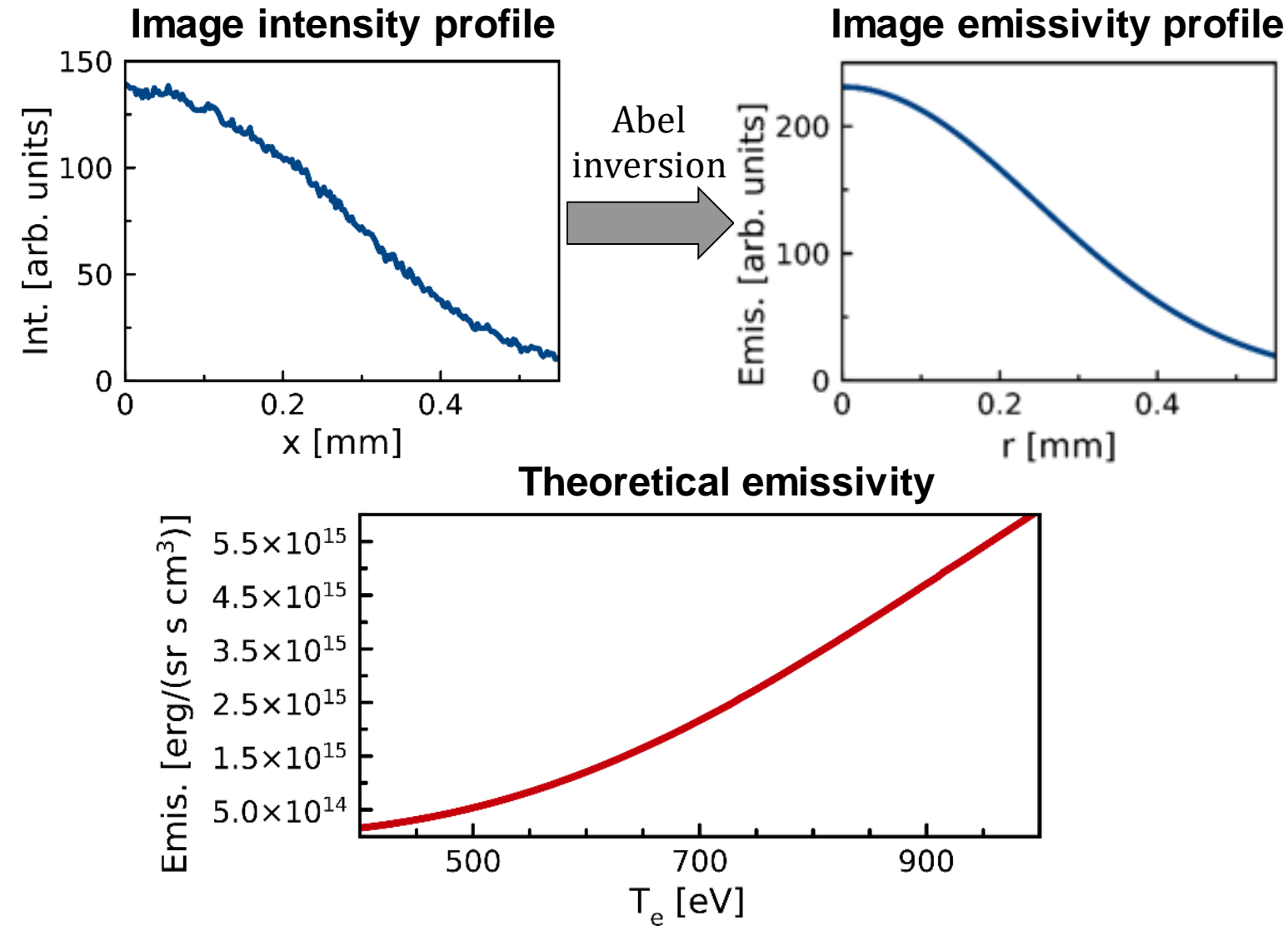
H50
B = 8.5T

H51
B = 0T

- Synthetic spectra for various temperatures were created
- Each spatially resolved spectrum was compared with synthetic spectra to extract T_e
- Account for spectral resolution by convolving with a Gaussian
- **Magnetic field and window thickness largely affect the temperature distribution**



Multi-objective data analysis enables $T_e(r,z)$ extraction



- Multi-objective data analysis permits extraction of **spatial distribution** of plasma conditions¹⁻⁴
- Simultaneous and self-consistent analysis of x-ray spectrum and narrow band image data¹
- Two alternative implementations produce consistent results
 - Forward reconstruction driven by a Pareto genetic algorithm
 - Quasi-analytic method in the optically thin approximation
- A collection of emissivity equations can be solved to get $T_e(r,z)$
- Emissivity weighted average of $T_e(r,z)$ is constrained with $T_e(z)$ from analysis of axially resolved spectra³

¹K. R. Carpenter et al, APS DPP contributed talk, October 2017, Milwaukee, WI

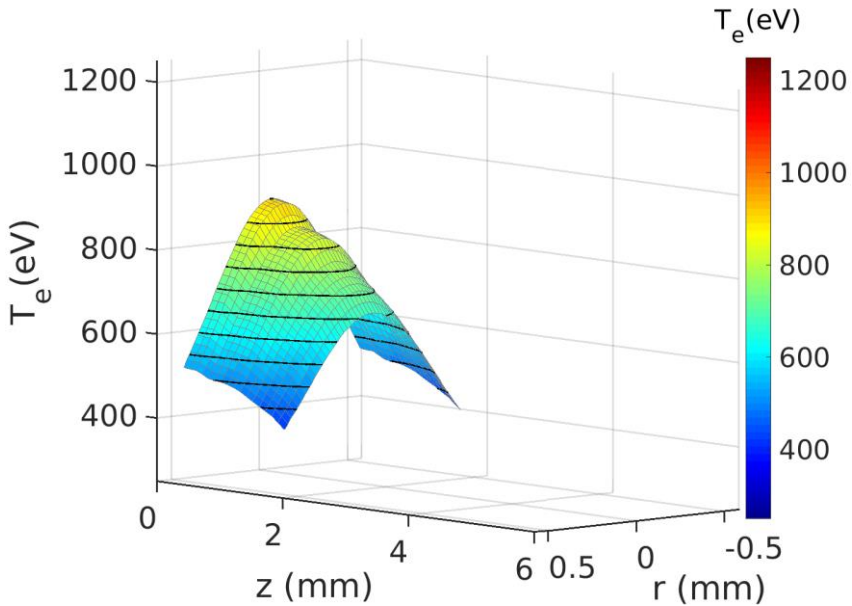
³L. A. Welser-Sherrill, R. C. Mancini, et al, Physical Review E **76**, 056403 (2007)

²I. Golovin, R. Mancini et al Physical Review Letters **88**, 045002 (2002)

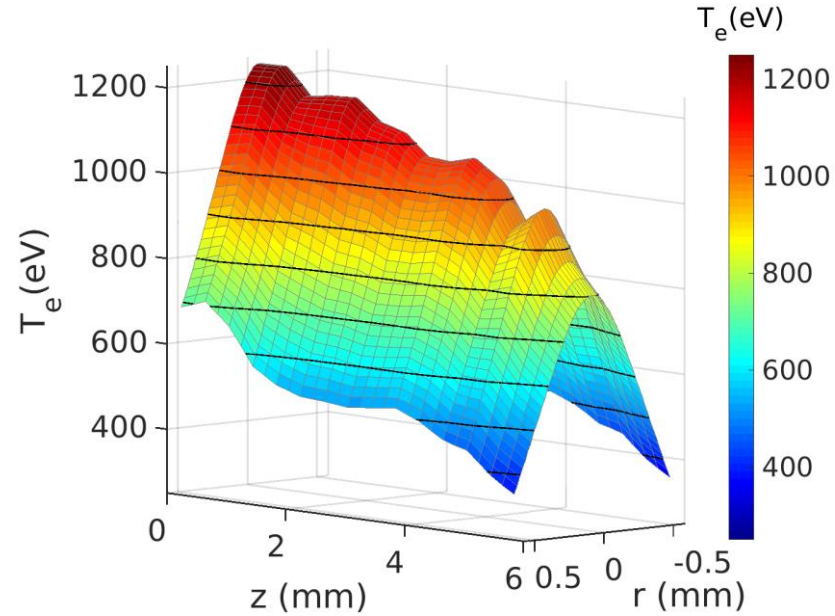
⁴T. Nagayama, R. Mancini et al Physics of Plasmas **19**, 082705 (2012)

$T_e(r,z)$ was extracted for three experiments

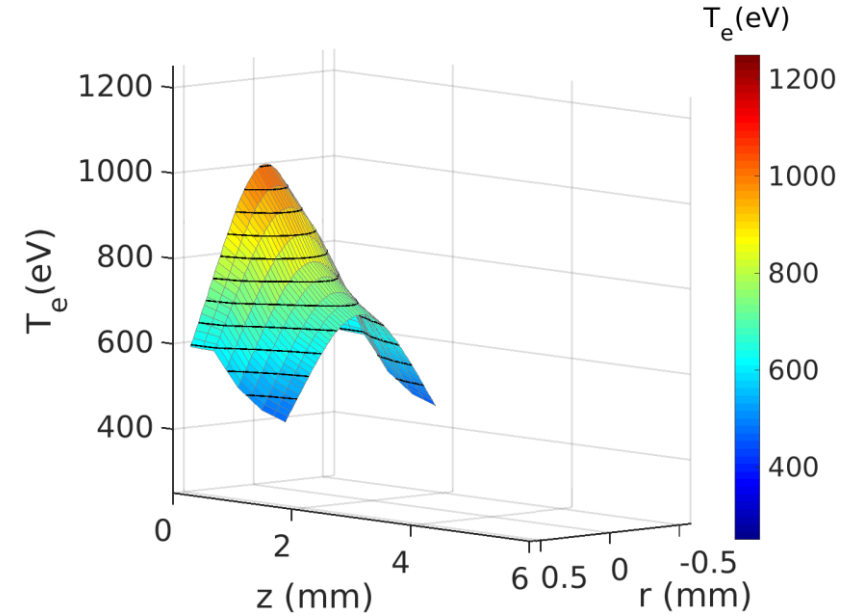
H45: B=8.5T, 3.4 μ m window



H50: B=8.5T, 1.77 μ m window



H51: B=0T, 1.77 μ m window



- H50 was hotter and had a longer emission column than H45 and H51
- $T_e(r,z)$ is dependent on the window thickness and external magnetic field
- The results from H45 and H51 show qualitative similarities, though the experimental parameters were quite different

$T_e(r,z)$ can be used to determine the experimental heat flux

Heat flux due to thermal conduction according to Braginskii¹:

$$\text{Electrons: } \vec{q}_e = -\chi_{\parallel}^e \vec{\nabla}_{\parallel} T_e - \chi_{\perp}^e \vec{\nabla}_{\perp} T_e - \chi_{\Lambda}^e (\hat{B} \times \vec{\nabla} T_e)$$

$$\text{Ions: } \vec{q}_i = -\chi_{\parallel}^i \vec{\nabla}_{\parallel} T_i - \chi_{\perp}^i \vec{\nabla}_{\perp} T_i - \chi_{\Lambda}^i (\hat{B} \times \vec{\nabla} T_i)$$

$\chi_{\parallel}^e, \chi_{\parallel}^i$ are functions of T and n

$\chi_{\perp}^e, \chi_{\perp}^i, \chi_{\Lambda}^e, \chi_{\Lambda}^i$ are functions of T, n, and B

Details and Approximations:

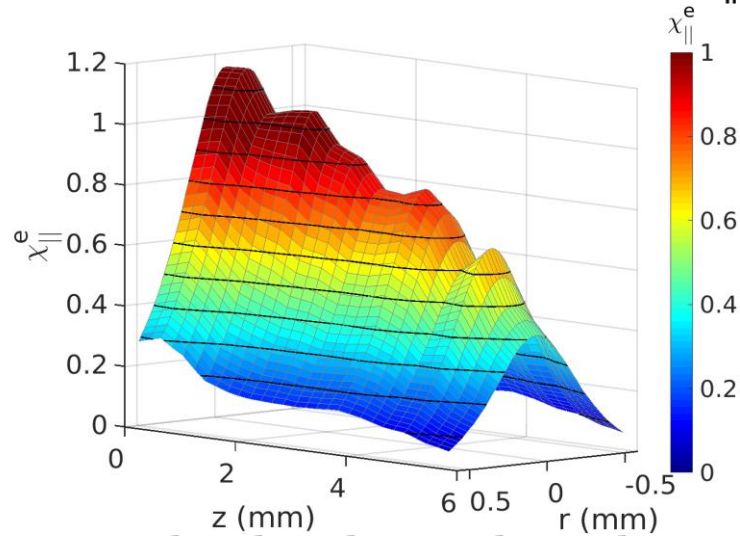
- Assume no fluid motion:
 $V_e = V_i = 0$
- Assume $T_e = T_i$
- Used coefficients for a deuterium (Z=1) plasma
- Effect of Ar tracer has not yet been considered
- Azimuthally directed, cross-field component of flux not yet evaluated
- ∇T determined with finite differences approximation

¹S. I. Braginskii, *Reviews of Plasma Physics* (Consultants Bureau, New York, 1965), Vol. 1, p. 205

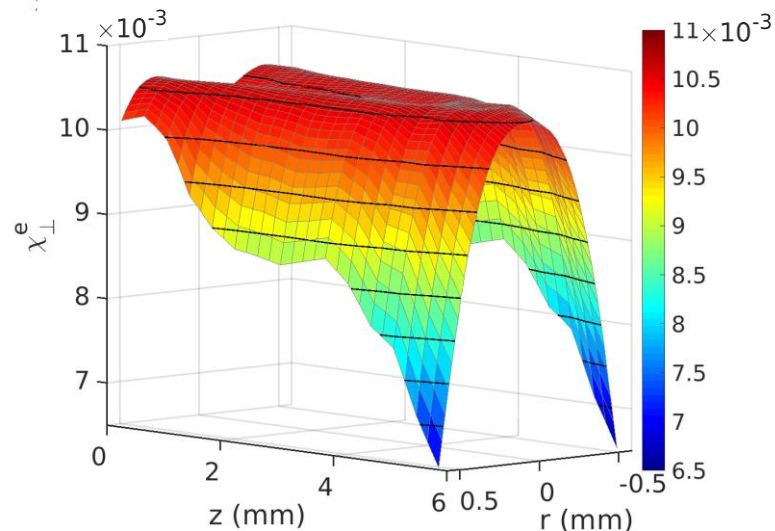
Electron thermal conductivity varies with B

H50 (B = 8.5T)

Parallel thermal conductivity, χ_{\parallel}^e

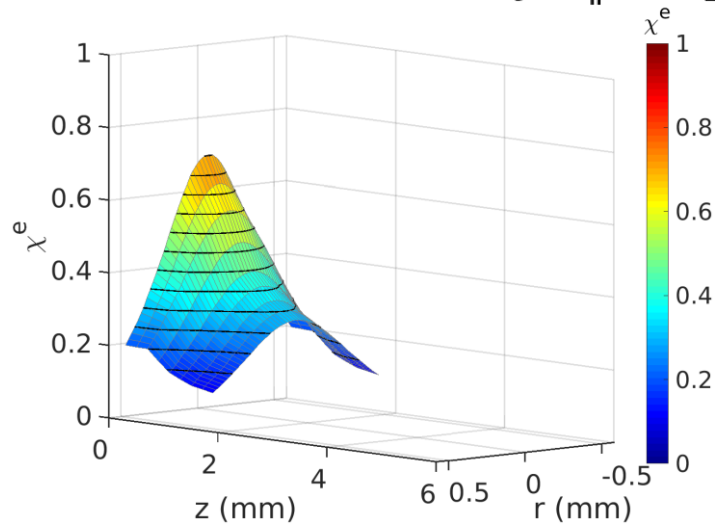


Perpendicular thermal conductivity, χ_{\perp}^e



H51 (B = 0T)

Thermal conductivity, $\chi_{\parallel} = \chi_{\perp}$



$$q_r^e = -\chi_{\perp}^e \frac{\partial T_e}{\partial r} \quad q_z^e = -\chi_{\parallel}^e \frac{\partial T_e}{\partial z}$$

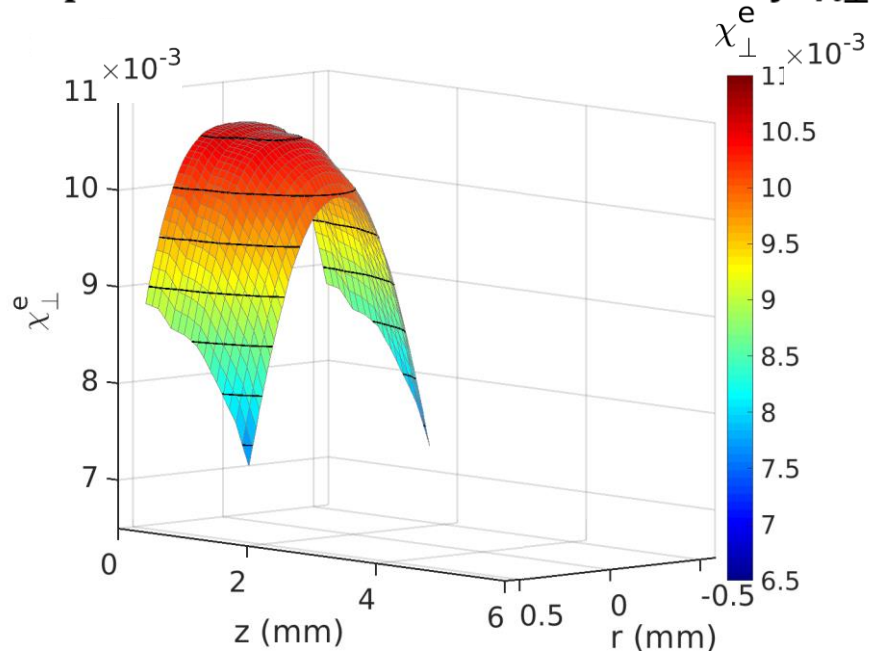
$$\vec{q}^e = q_r^e \hat{r} + q_z^e \hat{z}$$

Multiply conductivities by $1 \times 10^{30} \text{ s}^{-1} \cdot \text{m}^{-1}$ to get actual values

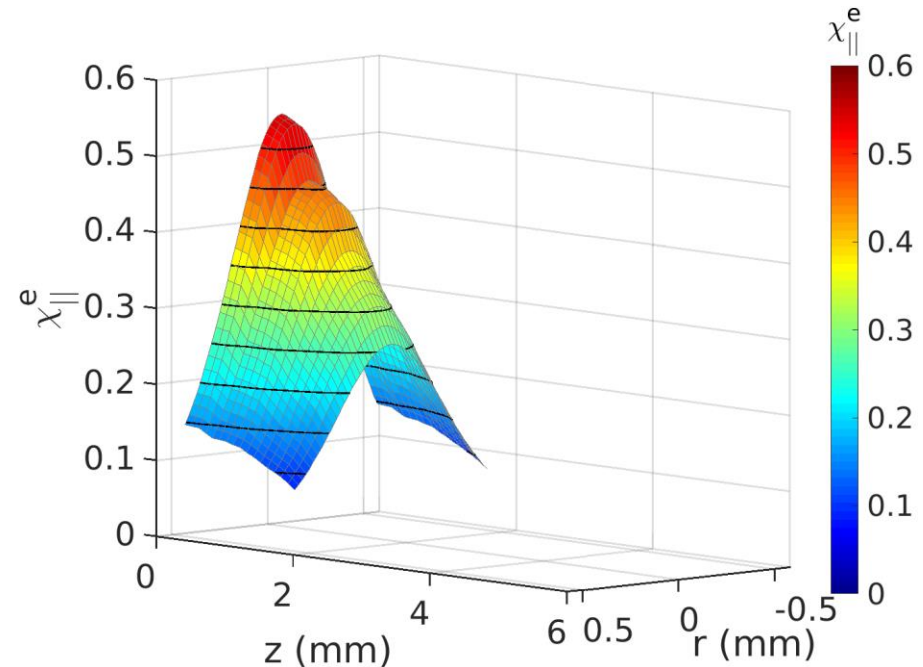
- Perpendicular thermal conductivity is 2-3 orders of magnitude lower than the parallel component
- Without B perpendicular and parallel conductivities are identical, i.e. thermal transport is isotropic

Magnetic field had similar effect in H45 (B=8.5T)

Perpendicular thermal conductivity, χ_{\perp}^e



Parallel thermal conductivity, χ_{\parallel}^e



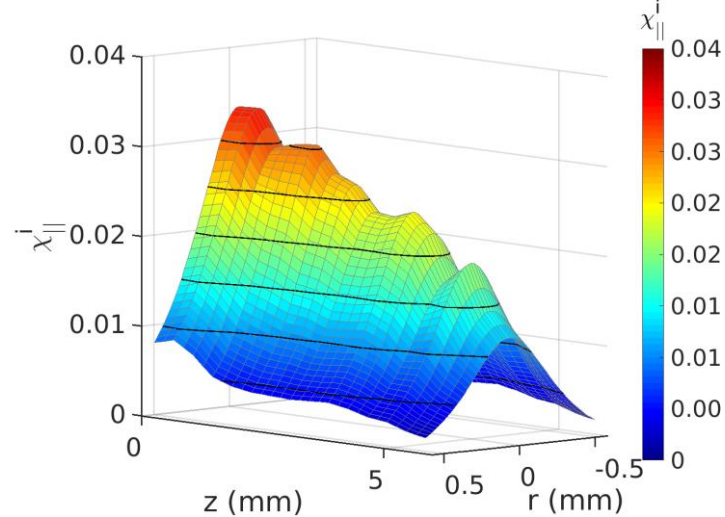
- Perpendicular conductivity in H45 is similar to H50 in both the magnitude and distribution of values
- Parallel conductivities are slightly smaller in H45 due to the lower temperature
- Thicker window used in H45 resulted in a shorter emission column and lower T_e (less laser energy coupling to fuel)

Multiply conductivities by $1 \times 10^{30} \text{ s}^{-1} \cdot \text{m}^{-1}$ to get actual values

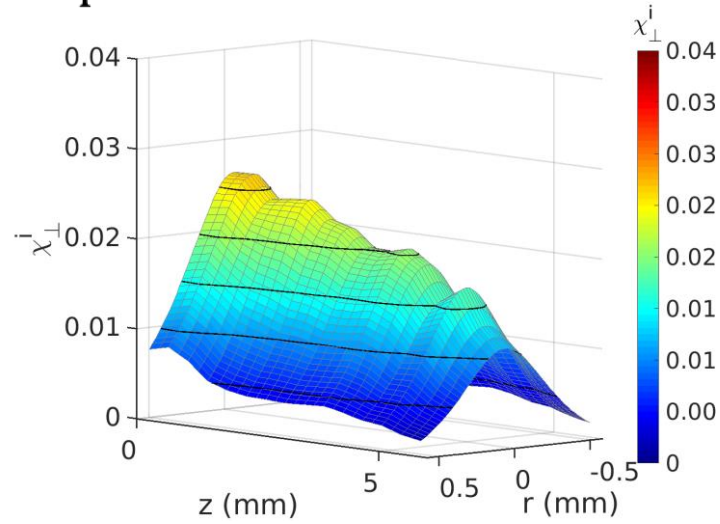
Ion thermal conductivity is not as sensitive to B

H50 (B = 8.5T)

Parallel thermal conductivity, χ_{\parallel}^i

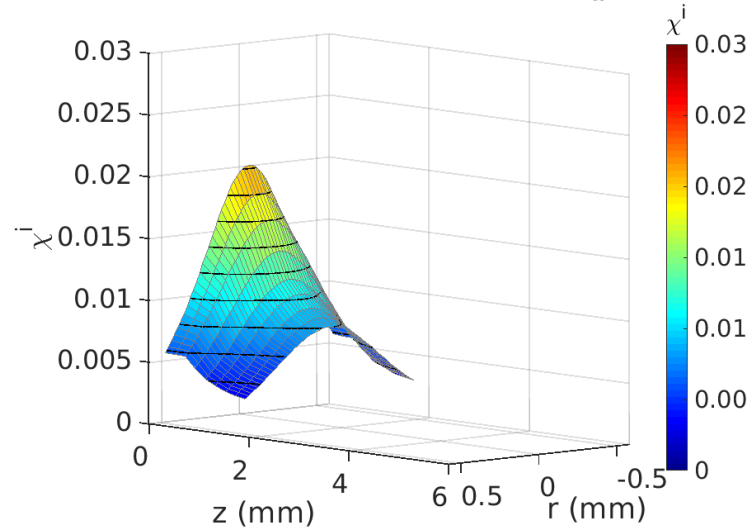


Perpendicular thermal conductivity, χ_{\perp}^i



H51 (B = 0T)

Thermal conductivity, $\chi_{\parallel} = \chi_{\perp}$



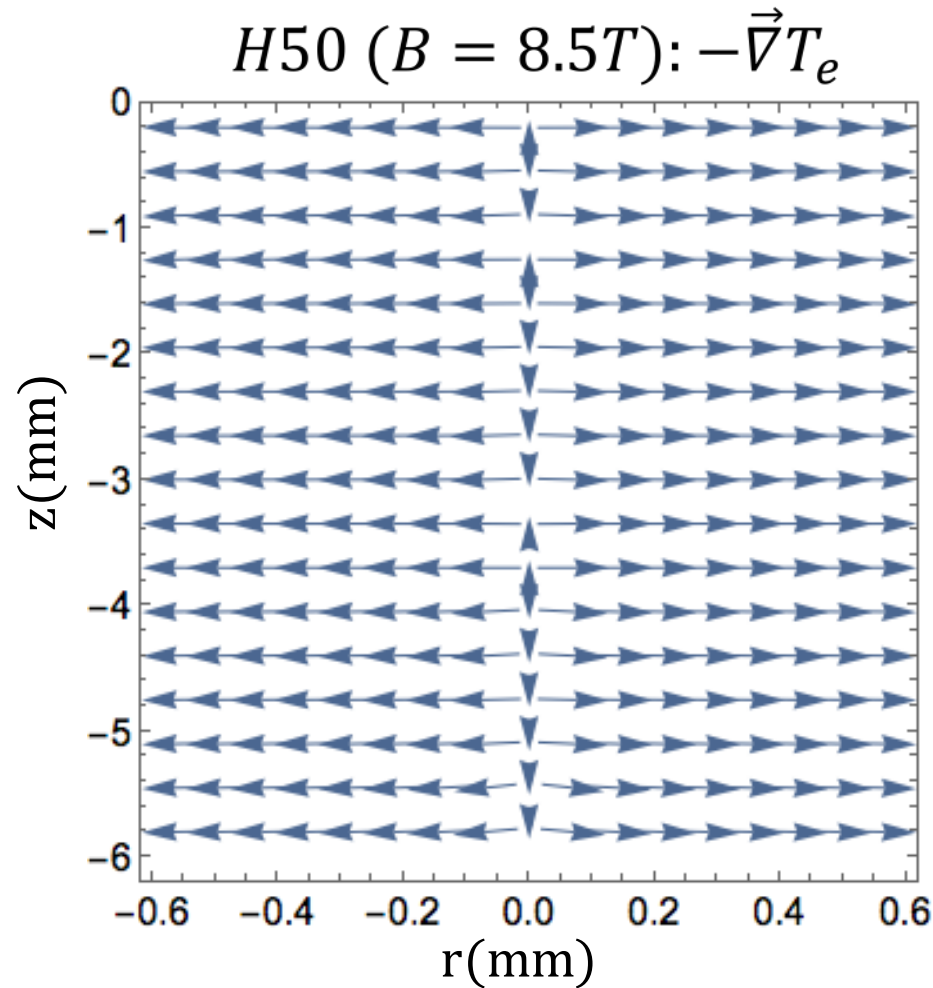
Multiply conductivities by $1.0 \times 10^{30} \text{ s}^{-1} \cdot \text{m}^{-1}$ to get actual values

- Assume $T_i = T_e$
- Ion thermal conductivity values are one order of magnitude smaller than electrons
- Magnetic field has less of an effect on ions
- Values are similar between the magnetic field and no magnetic field cases

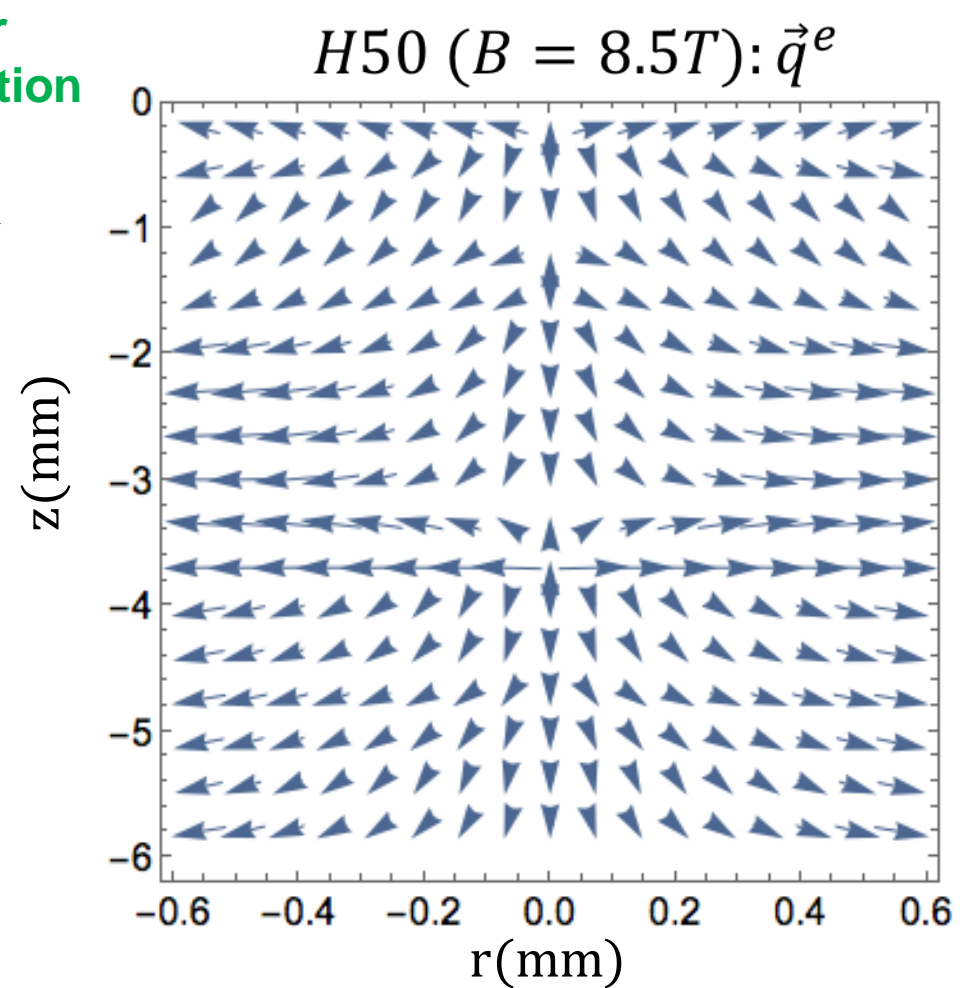
$$q_r^i = -\chi_{\perp}^i \frac{\partial T_i}{\partial r} \quad q_z^i = -\chi_{\parallel}^i \frac{\partial T_i}{\partial z}$$

$$\vec{q}^i = q_r^i \hat{r} + q_z^i \hat{z}$$

Electron heat flux: H50

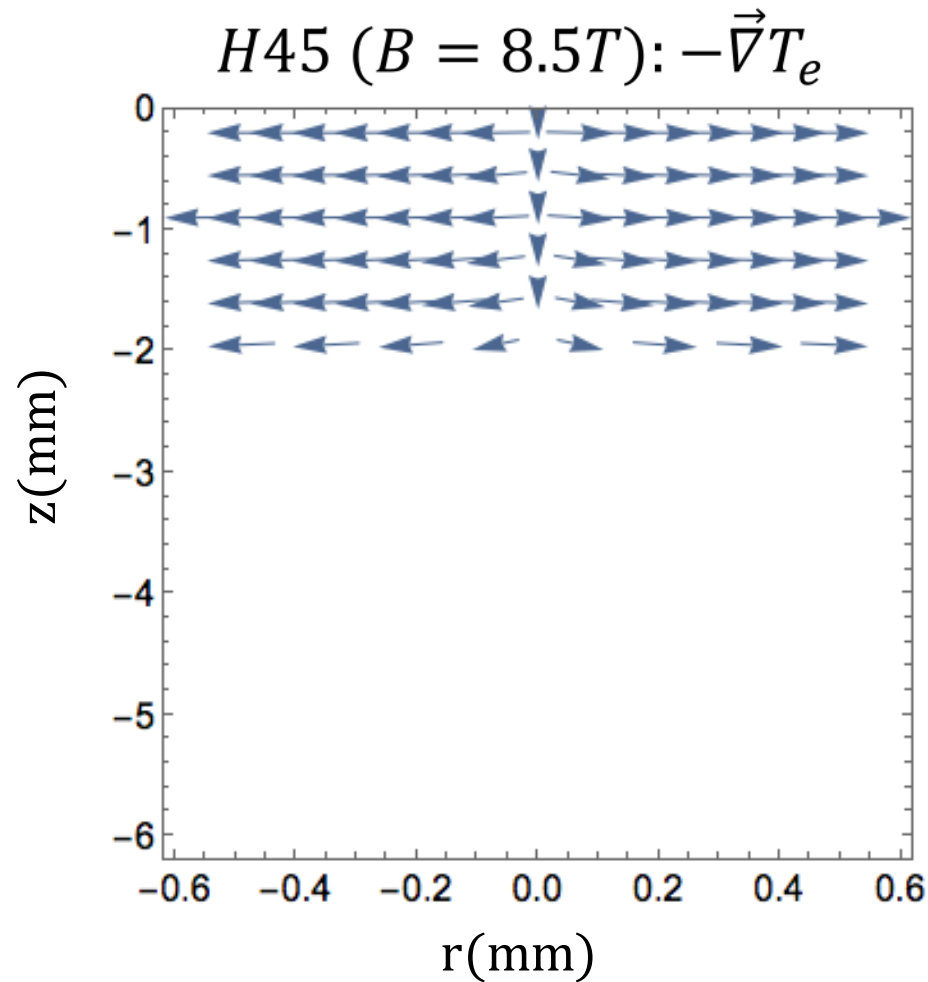


Laser
propagation

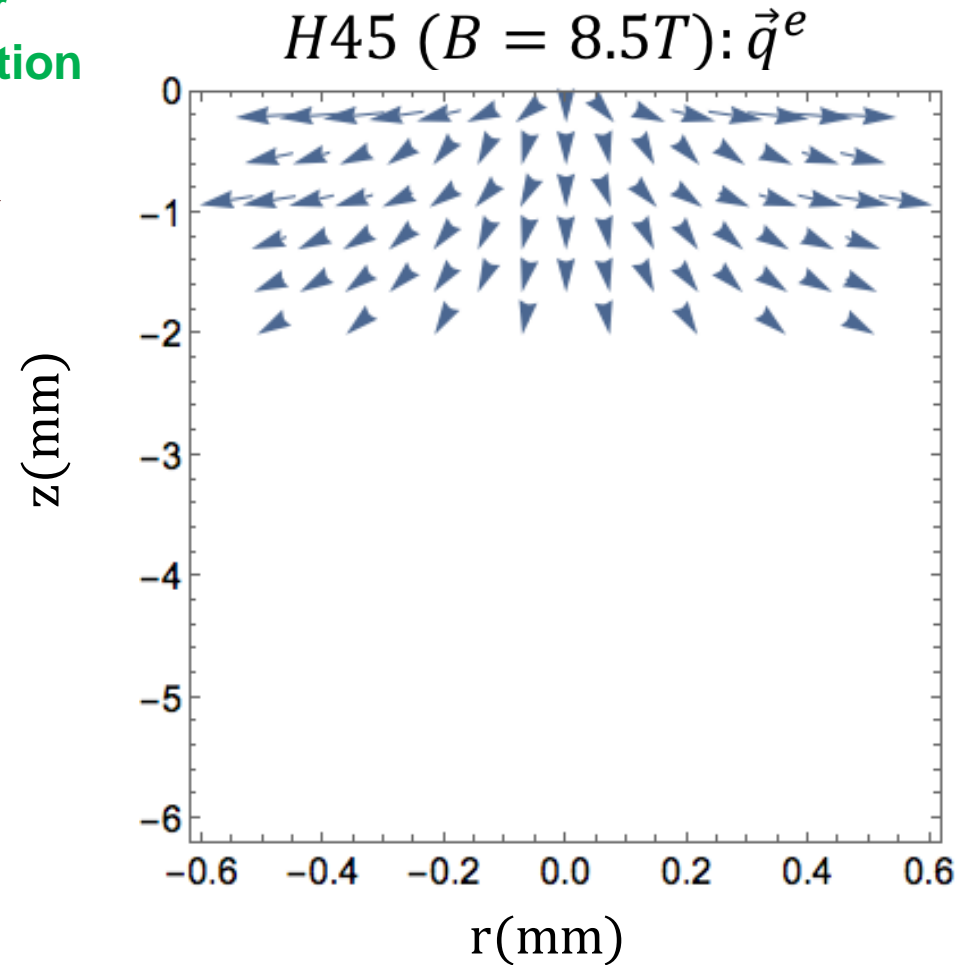
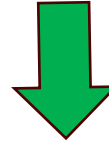


- Gradient found with finite differences approximation
- Temperature gradient is predominantly radial
- Near the center, the effect of the B-field results in a flux that is mostly axial

Electron heat flux: H45



Laser
propagation



- Similar to H50, the temperature gradient is largely radial
- The magnetic field effect on the electrons produces an electron heat flux with large axial components

Conclusions

- We have analyzed time-integrated spectrum and narrowband image data from laser heating experiments relevant to MagLIF, done with/without B field
- Using multi-objective data analysis we have extracted 2-D resolved temperature distributions, $T_e(r,z)$, for three experiments: H45(B=8.5T), H50(B=8.5T), H51(B=0T)
- LEH window thickness and magnetic field had prominent effects on the resultant distributions
- Using the formalism of Braginskii, we used $T_e(r,z)$ to examine the experimental heat flux due to electron and ion thermal conduction
- The magnetic field significantly reduces the radial heat flow
- Thermal conductivity of electrons is more largely affected by B-field than that of ions
- It is important now to compare data analysis results with simulations
- **The analysis can be performed on time-resolved data which would help unfold the time history of the distribution of temperature and thermal heat flow**
- **Still, time-integrated data analysis does show the B effect on heat flow**

This work is supported through a contract with Sandia National Laboratories

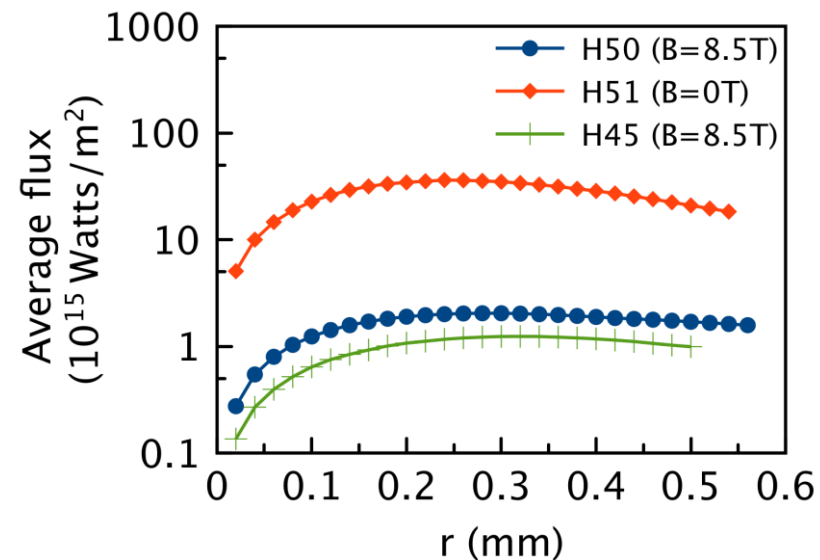
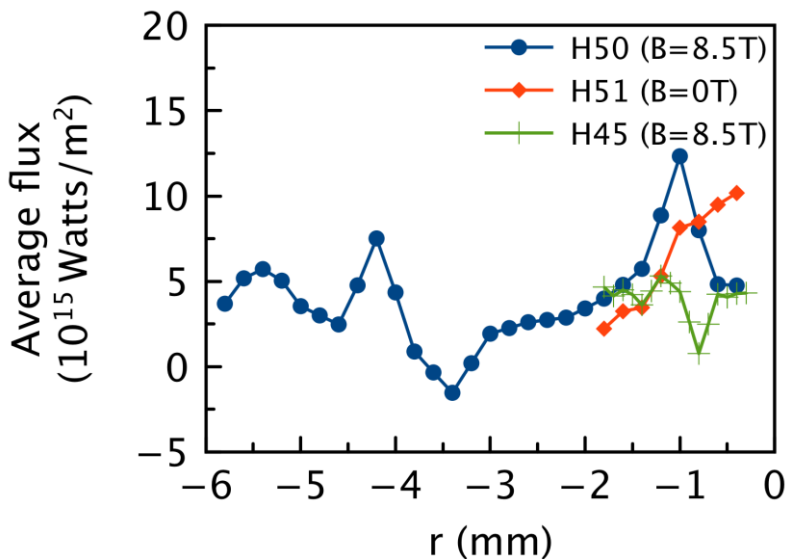
Extra slides

Temporally and spatially averaged flux

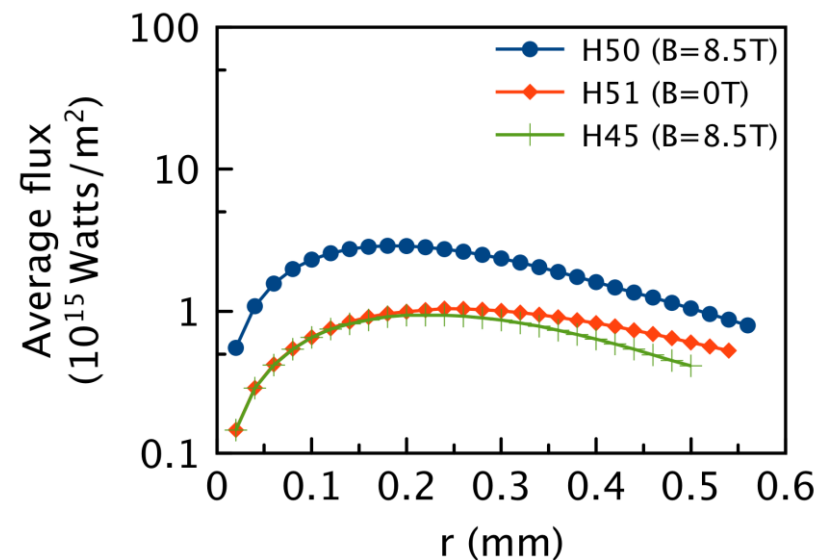
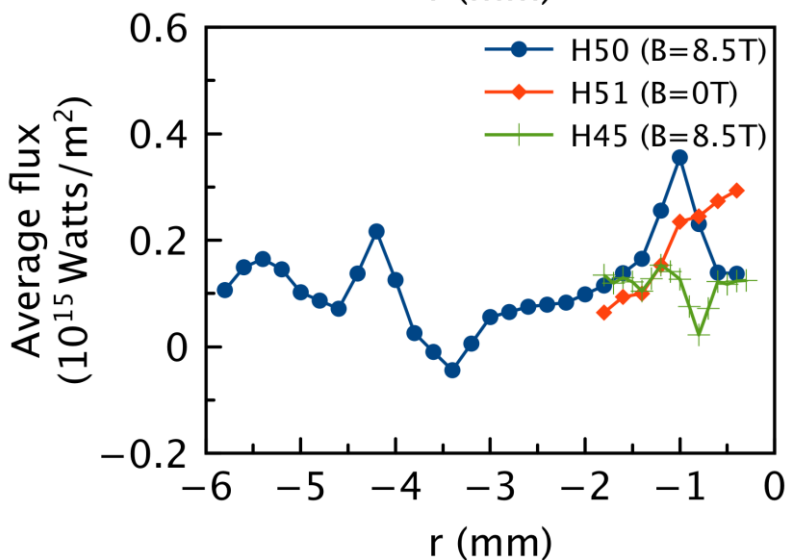
$$\langle q \rangle_z(z) = \frac{2\pi \int q_z(r, z) r dr}{2\pi \int r dr}$$

$$\langle q \rangle_r(r) = \frac{2\pi r \int q_r(r, z) dz}{2\pi r \int dz}$$

Electrons



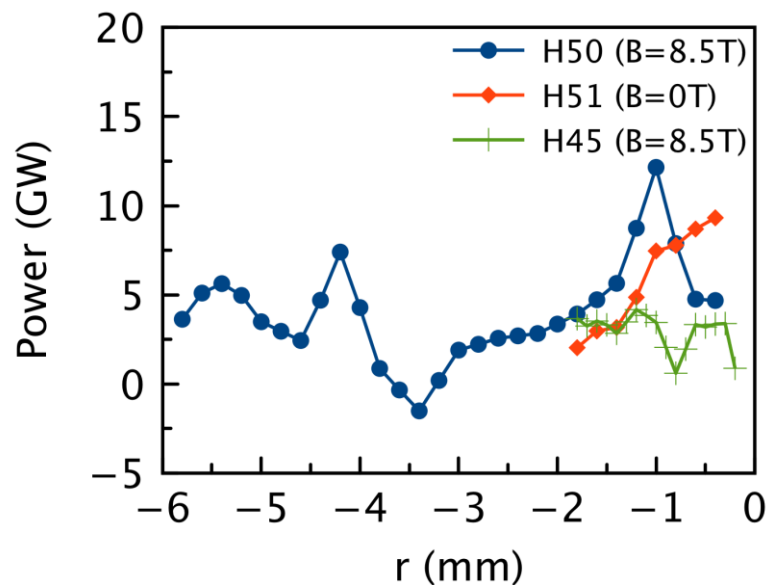
Ions



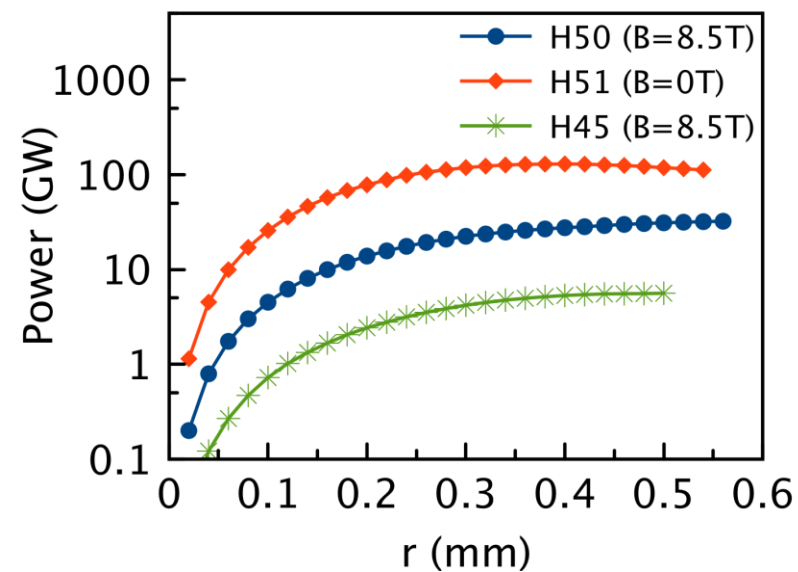
Time averaged energy flow

Electrons

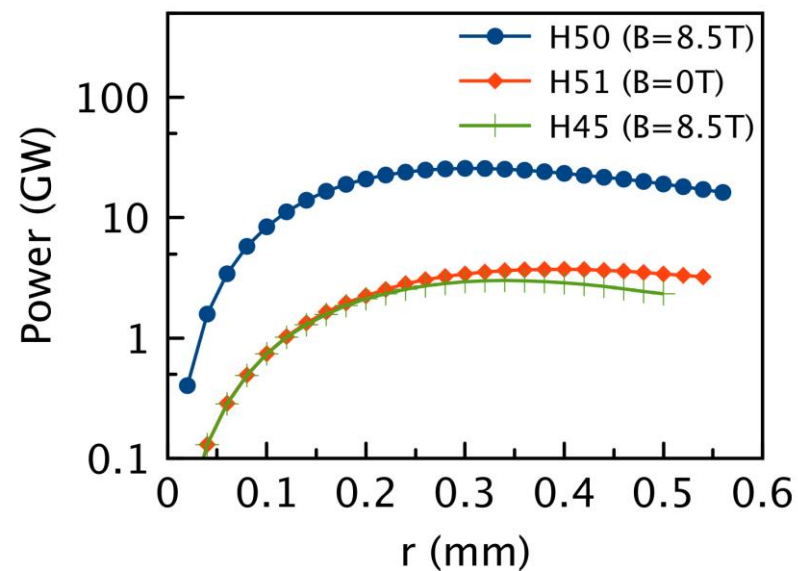
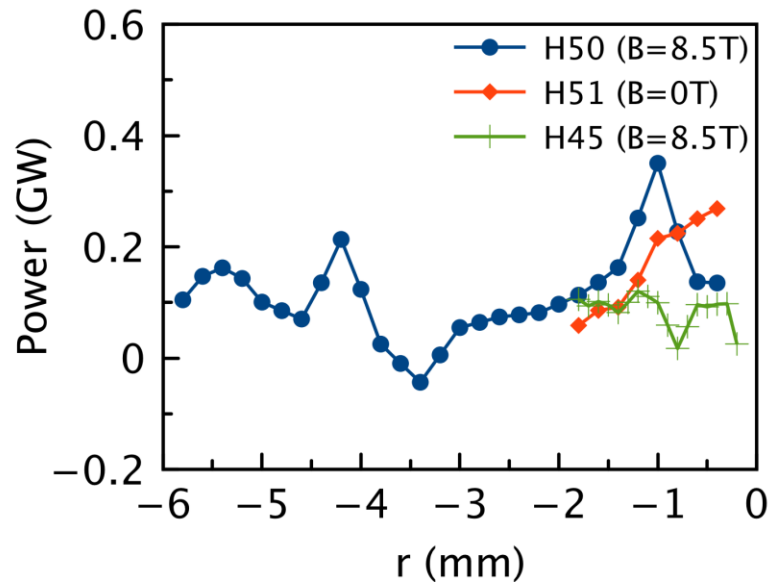
$$P_z(z) = 2\pi \int q_z(r, z) r dr$$



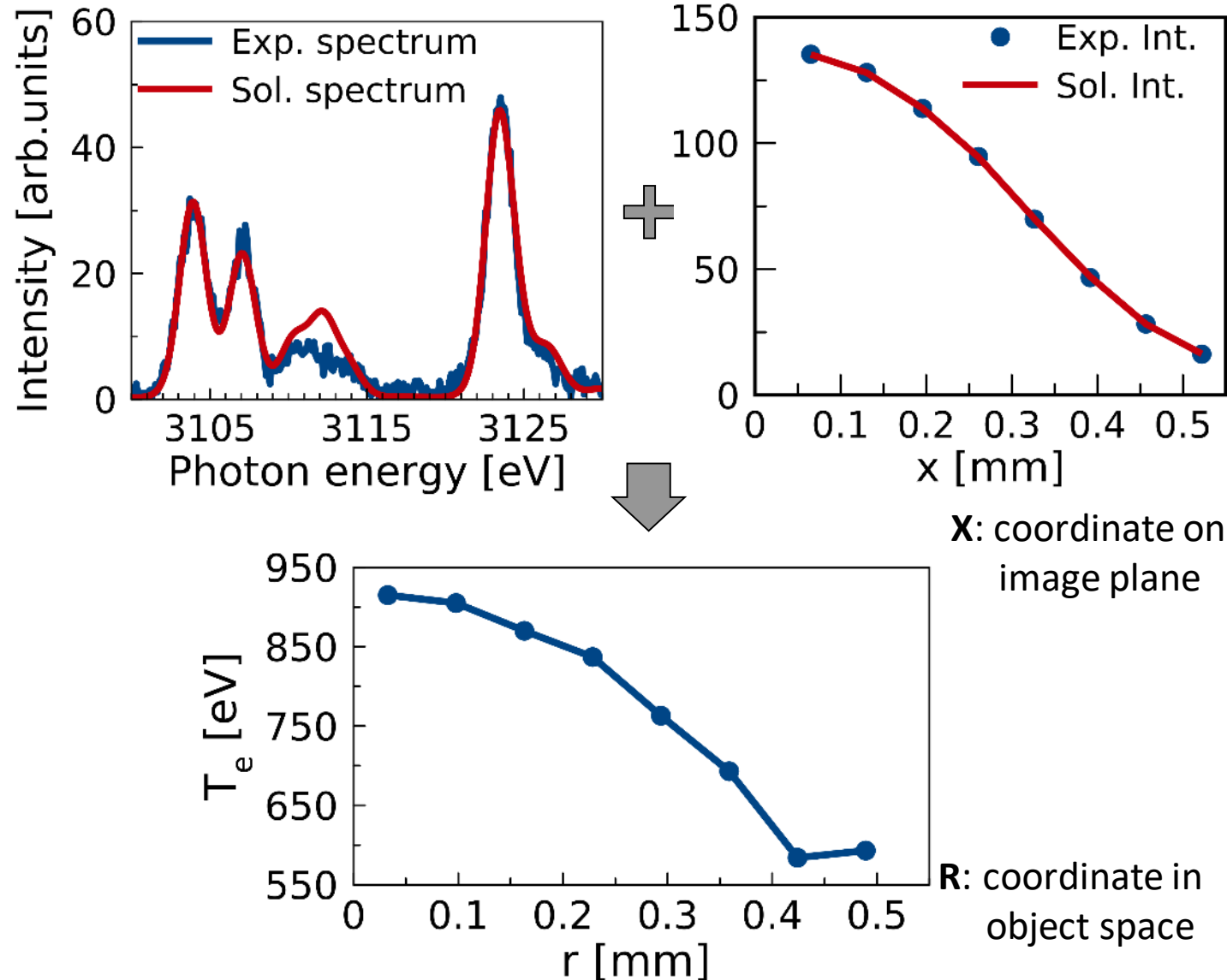
$$P_r(r) = 2\pi r \int q_r(r, z) dz$$



Ions



Two objective analysis produces $T_e(r,z)$



- Method is based on forward reconstruction
- Multi-objective optimization driven by a Pareto genetic algorithm (PGA) is performed
- Search for solutions that produce the best simultaneous and self-consistent approximations to both pieces of data
- This technique has previously been implemented to extract the spatial structure of implosion cores^{1,2}

¹I. Golovkin, R. Mancini, S. Louis, Y. Ochi, K. Fujita, H. Nishimura, H. Shirga et al, Physical Review Letters **88**, 045002 (2002)

²R. Mancini, Ch. 15 in "Applications of Multi-Objective Evolutionary Algorithms", Eds. C. Coello-Coello and G. Lamont, World Scientific Pub. ISBN 981-256-106-4 (2004)